



Expected Investigation of the (65803) Didymos–Dimorphos System Using the RGB Spectrophotometry Data Set from the LICIACube Unit Key Explorer (LUKE) Wide-angle Camera

Giovanni Poggiali^{1,2} , John R. Brucato¹ , Pedro H. Hasselmann³, Simone Ieva³ , Davide Perna³ , Maurizio Pajola⁴ , Alice Lucchetti⁴, Jasinghege D. P. Deshapriya³, Vincenzo Della Corte⁵, Elena Mazzotta Epifani³, Alessandro Rossi⁶ , Stavro L. Ivanovski⁷ , Angelo Zinzi⁸ , Andrea Meneghin¹, Marilena Amoroso⁸, Simone Pirrotta⁸, Gabriele Impresario⁸, Elisabetta Dotto³, Ivano Bertini^{5,9}, Andrea Capannolo¹⁰, Gabriele Cremonese⁴ , Biagio Cotugno¹¹, Massimo Dall’Ora¹² , Valerio Di Tana¹¹, Igor Gai¹³, Michèle Lavagna¹⁰, Federico Miglioretti¹¹, Dario Modenini^{13,14}, Pasquale Palumbo^{5,9} , Emanuele Simioni⁴, Simone Simonetti¹¹, Paolo Tortora^{13,14}, Marco Zannoni^{13,14}, and Giovanni Zanotti¹⁰

¹ INAF–Osservatorio Astrofisico di Arcetri, Firenze, Italy; giovanni.poggiali@inaf.it

² LESIA–Observatoire de Paris, Université PSL, CNRS, Sorbonne Université, Université de Paris, France

³ INAF–Osservatorio Astronomico di Roma, Porzio Catone (Roma), Italy

⁴ INAF–Osservatorio Astronomico di Padova, Padova, Italy

⁵ Istituto di Astrofisica e Planetologia Spaziali, Istituto Nazionale di Astrofisica, Rome, Italy

⁶ IFAC-CNR, Firenze, Italy

⁷ INAF–Osservatorio Astronomico di Trieste, Trieste, Italy

⁸ Agenzia Spaziale Italiana, Roma, Italy

⁹ Università degli Studi di Napoli “Parthenope”, Dipartimento di Scienze & Tecnologie, Napoli, Italy

¹⁰ Politecnico di Milano, Dipartimento di Scienze e Tecnologie Aerospaziali, Milano, Italy

¹¹ Argotec, Torino, Italy

¹² INAF–Osservatorio Astronomico di Capodimonte, Napoli, Italy

¹³ Alma Mater Studiorum–Università di Bologna, Dipartimento di Ingegneria Industriale, Forlì, Italy

¹⁴ Alma Mater Studiorum–Università di Bologna, Centro Interdipartimentale di Ricerca Industriale Aerospaziale, Forlì, Italy

Received 2022 February 6; revised 2022 May 20; accepted 2022 June 6; published 2022 July 15

Abstract

The Light Italian Cubesat for Imaging of Asteroids (LICIACube) is part of the NASA Double Asteroid Redirection Test (DART), the first mission aiming to demonstrate the applicability of the kinetic impactor method for planetary defense. The mission was launched on 2021 November 24 to perform the impact experiment on Dimorphos, the small secondary of the binary asteroid (65803) Didymos. The 6U LICIACube, stored as a piggyback of the DART spacecraft, is the first Italian mission operating in deep space managed by the Italian Space Agency that will witness the effects of the DART impact on Dimorphos. On board LICIACube, there is a suite of cameras that will perform imaging of Didymos and Dimorphos to investigate the DART impact effects and study the binary system. Among them, the LICIACube Unit Key Explorer (LUKE), a wide-angle camera coupled to an RGB Bayer pattern filter, will be pivotal to constrain the surface composition and heterogeneity of the binary system due to differences in surface properties linked with possible space weathering effects and/or the presence of exogenous material. Multiband photometric analysis of LUKE data and laboratory experiments in support of data interpretation will provide new insights on the binary asteroid nature and evolution. Moreover, photometric phase curve analysis will reveal the scattering properties of the granular surface medium providing important constraints for the microphysical properties of the Didymos–Dimorphos system. In this work, we will present the state of the art of the LUKE scientific activities with an overview of the instrument setup, science operations, and expected results.

Unified Astronomy Thesaurus concepts: Asteroids (72); Near-Earth objects (1092); Multivariate analysis (1913); Laboratory astrophysics (2004); Phase angle (1217); RGB photometry (1397); Near infrared astronomy (1093)

1. Introduction

The NASA Double Asteroid Redirection Test (DART; Cheng et al. 2018; Rivkin et al. 2021), launched on 2021 November 24 from Vandenberg Space Force Base (California, USA), is the first mission to perform a kinetic impact deflection test on a celestial body. The spacecraft is en route to encounter the binary asteroid (65803) Didymos with the aim to impact Dimorphos, the smaller moonlet of the binary system. The spacecraft mass of 550 kg and the impact velocity of about 6.6 km s^{−1} were estimated to be sufficient to change the binary

orbital period of Dimorphos by about 10 minutes; hence, differences in the orbital period due to the impact will be measured by ground-based telescopes shortly after the impact.

The Light Italian Cubesat for Imaging of Asteroids (LICIACube; Dotto et al. 2021) is carried as a secondary spacecraft by DART and will be released about 10 days before the impact. The Italian cubesat will perform an autonomous flyby of the binary system with several scientific objectives: (i) to directly witness the impact of the DART spacecraft on Dimorphos’s surface; (ii) to study the ejecta plume over its evolution in time and under varied phase angles in order to estimate the properties of the plume and the evolution of its grain distribution; (iii) to study the impact site with sufficient resolution to allow measurements of the size, color, and morphology of the artificial crater formed in the aftermath; and



Original content from this work may be used under the terms of the [Creative Commons Attribution 4.0 licence](https://creativecommons.org/licenses/by/4.0/). Any further distribution of this work must maintain attribution to the author(s) and the title of the work, journal citation and DOI.

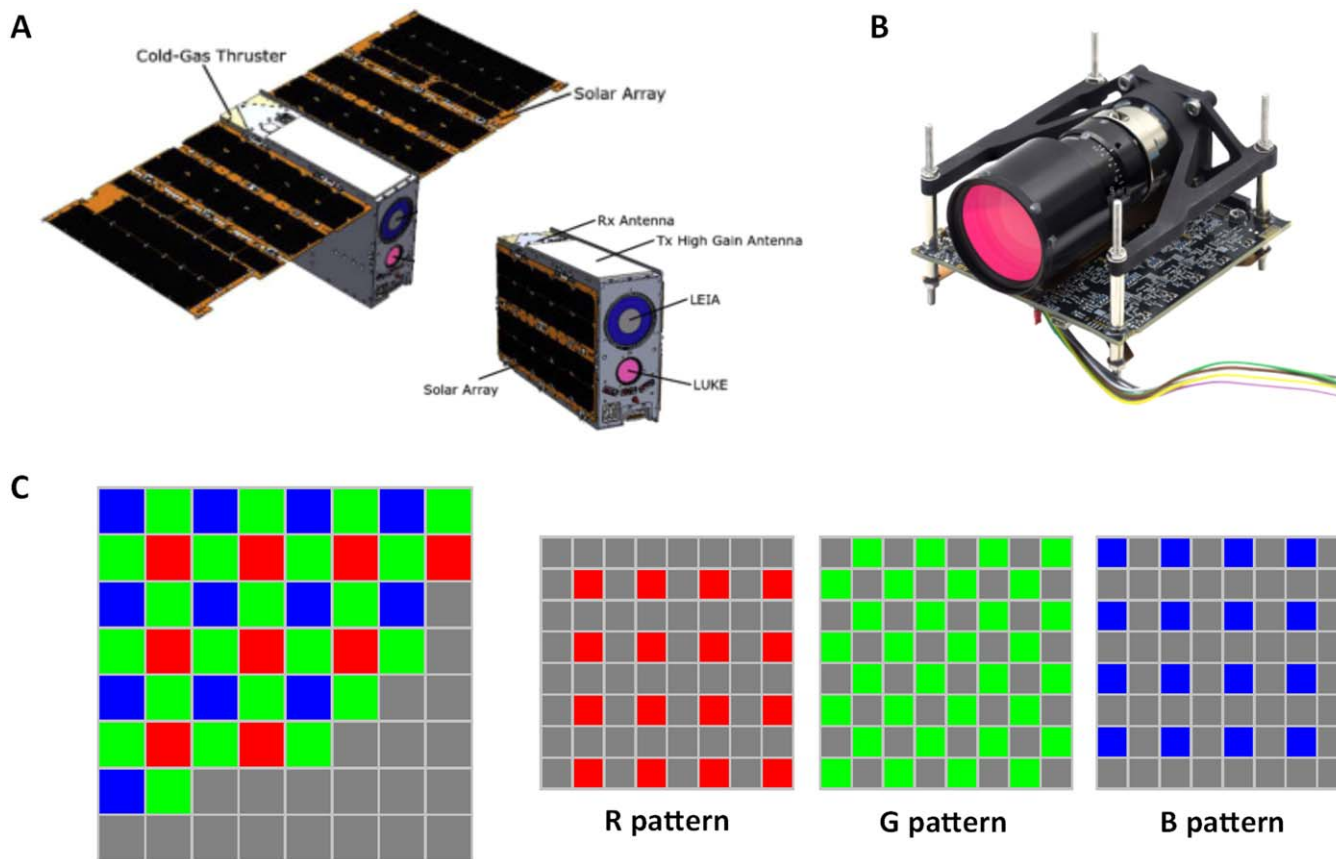


Figure 1. (a) A 3D model of LICIACube with the solar array deployed and closed. Labels mark some of the main components of the spacecraft and the position of two payloads, LEIA and LUKE, on board the spacecraft; adapted from Dotto et al. (2021). (b) Picture of the LUKE Gecko Imager for cubesat from SCS Space (www.scs-space.com). (c) LUKE RGB Bayer pattern filter scheme and scheme of single color patterns.

(iv) to perform observations of the nonimpacted hemisphere to increase accuracy in the determination of the target's shape and volume and for overall investigation of the surface. To fulfill such key objectives, LICIACube is carrying a suite of cameras composed of the LICIACube Explorer Imaging for Asteroid (LEIA), a narrow field-of-view (FoV) camera, and the LICIACube Unit Key Explorer (LUKE), a wide FoV imager with an RGB Bayer pattern filter (Figure 1). DART and LICIACube are part of the Asteroid Impact & Deflection Assessment collaboration between NASA and ESA; data obtained by the two spacecraft will be complemented by the ESA HERA mission (Michel et al. 2018), to be launched in 2024 and arriving at the Didymos system in 2027, for a deeper characterization of the binary system and further investigation of the effects of the DART impact.

The Didymos system (provisional designation 1996 GT), the target of the DART-LICIACube mission, was discovered on 1996 April 11 by the University of Arizona Steward Observatory's Spacewatch survey from Kitt Peak Observatory. The secondary asteroid Dimorphos, the impact target of DART, was found with optical light-curve analysis and Arecibo radar imaging in 2003 and later confirmed as a low-obliquity and retrograde rotator (Scheirich & Pravec 2009). Nowadays, we know that almost 15% of the NEA population larger than 200 m is composed of binary systems (Pravec et al. 2006). The primary (Didymos) is a fast rotator of about 780 m in diameter with a spin period of 2.26 hr, an oblate shape, and an equatorial ridge. The secondary (Dimorphos) is approximately 163 m across and orbits around Didymos in 11 hr and 55 minutes. The

two asteroids are orbiting with a semimajor axis of 1.18 km. This binary system is the ideal test target for a Planetary Defense mission, since it poses no actual threat to Earth in the near future, and the momentum transferred by DART is not high enough to significantly change the orbit of the binary system around the Sun. In addition, a space mission to Didymos is a key opportunity to investigate the nature and origin of binary asteroids.

The color and reflectance properties of asteroids are pivotal to infer their compositions and investigate their evolutionary history. Indeed, differences in composition or space weathering alteration processes (such as bombardment by meteoroids and/or solar wind ions) drive variations in asteroids' spectral properties. Unveiling such differences is necessary to understand the origin and relative exposure age of surface units on primitive solar system objects. In the past years, color studies have been extensively used to investigate the surfaces of small bodies by means of analysis of data acquired in the visible spectral range. Various spectrophotometric analyses of the OSIRIS/Rosetta data of comet 67P/Churyumov-Gerasimenko, such as the multivariate statistical analysis (Perna et al. 2017) and others (Fornasier et al. 2015), showed clear differences between several regions of the comet and were fundamental to identifying and studying the temporal evolution of ice patches (Deshapriya et al. 2018), as well as constraining the composition and physical processes behind the emission of dust jets. The Hayabusa mission observed clear phase reddening on the S-type asteroid Itokawa with a direct implication for the taxonomic classification and the assessment

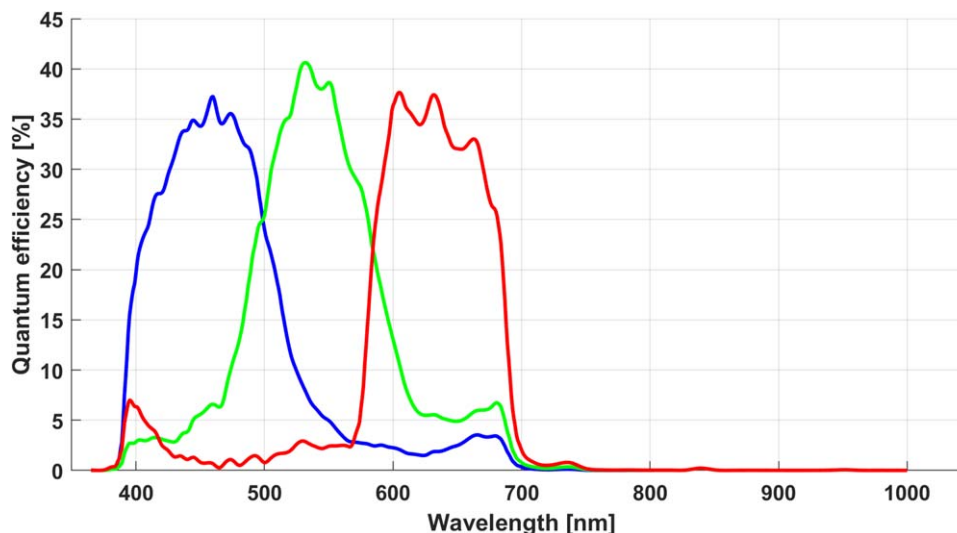


Figure 2. The RGB band efficiency of the LUKE camera.

of spectral characteristics, such as space weathering on the surface (Tatsumi et al. 2018). Moreover, the Itokawa spectral change is consistent with a very large variation in the degree of space weathering, suggesting the presence of resurfacing processes (Koga et al. 2018). Multicolor observations of asteroids belonging to the C-complex asteroid taxonomic class, like Ryugu by Hayabusa 2 (Sugita et al. 2019) and (101955) Bennu by OSIRIS-REx (DellaGiustina et al. 2020), improved the understanding of the nature and evolutionary path of these objects.

2. Instrument Overview and Planned Operations

Data from LUKE will be pivotal to perform color analysis and investigate any spectral differences in the Didymos system. LUKE is a Gecko imager provided by the SCS space company. The 70.55 mm focal length is designed to work in focus between 400 m and infinity. The FoV is $\pm 5^\circ$ and the Instantaneous FoV (IFoV) is $78 \mu\text{rad}/\text{px}$ with a spatial scale of about 4 m pixel^{-1} at 51 km. LUKE is equipped with a front-illuminated CMOS detector (ams CMV2000), the pixel pitch is $5.5 \mu\text{m}$, and images will be 1088×2048 pixels. It is an RGB camera with a Bayer pattern filter (Figure 1(C)). In Figure 2, the efficiencies for the RGB bands of LUKE are shown as declared by the producer. Moreover, the hardware is capable of directly integrating the image data to the integrated mass storage. LUKE observations will be downloaded as raw 8 bit images and processed by the calibration pipeline, including Bayer postprocessing using a standard debyerization algorithm as the first stage. Other algorithms will be tested as part of the calibration pipeline (Zinzi et al. 2022; v. Della Corte et al. 2022, in preparation). Communications with other subsystems will be allowed by the On-Board Computer and Data Handling of LICIACube; in particular, it will interface the payload and platform subsystems for Telemetry and Telecommand to properly manage the satellite and act as the satellite mass memory (Dotto et al. 2021). Several ground measurements with and without a calibrated integrating sphere as a light source were performed by the mission team before launch. The detector is near to linear response, and calibration data analysis is ongoing; mainly electric and radiometric camera calibration parameters will be retrieved. An in-flight calibration session is

foreseen, and the camera performance will be checked during the 10 day LICIACube cruise phase. In-flight calibration data will be downloaded before the start of the scientific acquisitions. Camera ground and in-flight calibration will be addressed in detail in a dedicated paper from Della Corte et al.

LICIACube will be released by DART about 10 days before the impact, and it will autonomously fly to the target, reaching a minimum distance of about 51 km (closest approach). During the flyby, both the LEIA and LUKE cameras will acquire 228 RGB images (for a simulated example, see Figure 3) of the impacted and nonimpacted target sides with a resolution ranging from 71 down to 4.3 m pixel^{-1} . At about 4 m pixel^{-1} resolution, being Didymos diameter about 780 m, the resultant diameter in pixels of the asteroid will be around 195 pixels, and the total area in pixels will be about 30,000 pixels, if it is uniformly illuminated (condition not expected). During the closest approach, LUKE will acquire 25 RGB images dedicated to surface investigation with a resolution lower than 8 m pixel^{-1} . The proximity operation and image acquisition at the asteroid have been scheduled on the basis of the trajectory design and orbit determination constraints to accomplish the different mission objectives (Dotto et al. 2021). Triplets will be acquired at 3 fps speed with different integration times; there will be no limitation on the choice of the integration times within the detector performances, and ideally, it will be up to 1 s (naturally, the choice will have an impact on the time between images). The LUKE final imaging timing can be modified before timeline execution; all of the images will be stored on board in payload memory, which determines the maximum number of images that could be acquired. In Table 1, we report the LUKE image acquisition plan.

In the next section, we report the expected results obtainable from images acquired by LUKE and the scientific analysis that will be performed on the overall LUKE data set, including the laboratory measurements foreseen to support their interpretation.

3. LUKE Expected Results and Scientific Activity

During the closest approach, LUKE will obtain images in the RGB filters of both the impacted and nonimpacted hemispheres

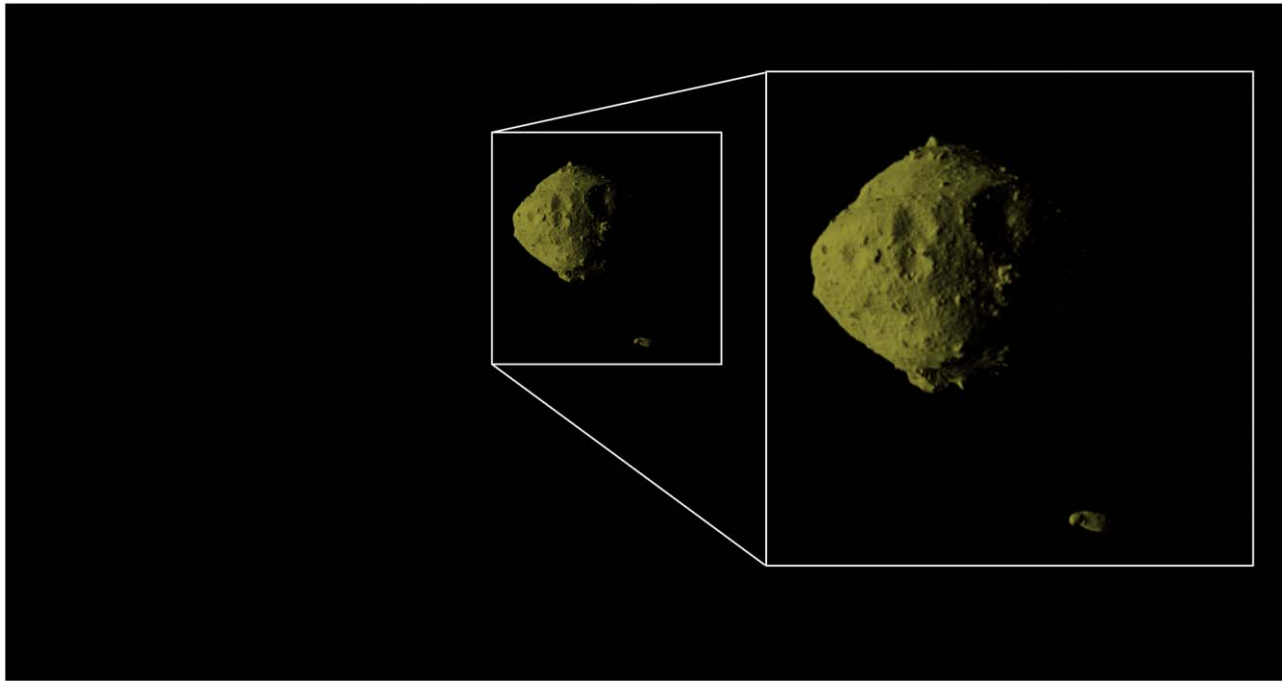


Figure 3. Original frame and zoom-in of analog image of Didymos–Dimorphos system, simulated using the shape models of asteroids Ryugu and Itokawa, as observed by the LUKE camera but not including a possible artifact induced by the Bayer filter. The image shows resolvable features on the surface that will allow geomorphological study of the system (Pajola et al. 2022, this issue). This image corresponds to a phase angle of around 50° and a distance from the target, Dimorphos, that is similar to the distance planned at the closest approach. The subtle butterscotch color of the Didymos–Dimorphos system, obtained considering the ground-based spectrum of the asteroid and the LUKE camera transmission filters, could appear to the human eye to be very similar to the color of the S-type asteroid 433 Eros visited by the NASA NEAR Shoemaker spacecraft.

Table 1

LUKE Camera Imaging Timing Tuned Considering Targets and Scientific Objectives

RGB Triplet Imaging Timing	Timeline after Nominal DART Impact
1 triplet every 6 s	Between 28 and 136 s
1 triplet every 3 s	Between 136 and 154 s
1 triplet every second	Between 154 and 179 s
1 triplet every 3 s	Between 179 and 194 s
1 triplet every 6 s	Between 194 and 320 s

of Dimorphos with a maximum spatial resolution of $\sim 4.3 \text{ m pixel}^{-1}$ (for both the raw and reconstructed RGB images). Spectrophotometric analyses will be used to investigate the surface composition of Dimorphos; spectrophotometric data will make it possible to investigate the surface heterogeneity at the observed scale and map the surface composition of the object, also looking for the possible presence of exogenous materials on the target surface due to collision with other asteroids during the evolution of the system (see Figure 4, last hypothesis and text below). The results of LUKE, joined with the LEIA and DRACO cameras, respectively, on board LICIACube and DART, will allow a detailed investigation of the geology of the Didymos–Dimorphos system (Pajola et al. 2022, this issue).

As recently shown by Hayabusa2’s Small Carry-on Impactor experiment (Arakawa et al. 2020), the comparison of the impacted and nonimpacted sides could give useful hints to investigate changes in the physical properties of the surface material induced by the shock and, in addition, decouple

impact effects from those induced by space weathering (Honda et al. 2021). Potentially, color differences in observations between Didymos and Dimorphos could also be indicative of different levels of space weathering originating from the binary system formation. Such data would be pivotal in helping in the investigation of binary asteroid evolution at large.

3.1. Multivariate Statistical RGB Data Analysis

Multivariate statistical analysis of data is a powerful technique in investigating small local variations in planetary surfaces. We will be using the G-mode multivariate statistical clustering analysis (Barucci et al. 1987; Gavrrishin et al. 1992; Barucci et al. 2005) on the spectrophotometric data acquired by LUKE to discern small local variations on Didymos’s and Dimorphos’s surfaces. This technique can be applied even when the spatial and/or magnitude scale of these variations is negligible in the global context (e.g., Perna et al. 2017; Barucci et al. 2019, 2020), and it can also be used successfully with three variables (Deshapriya et al. 2021). The G-mode analysis is indeed able to identify possible artifacts resulting from the reconstruction of the color image from the Bayer pattern image, similar to the way the pixels corresponding to shadows and cometary activity were identified by G-mode analysis of the nucleus of comet 67P (Perna et al. 2017). Using multicolor images acquired by LUKE, we will analyze the features on Dimorphos’s and Didymos’s surfaces from both a geomorphological and compositional perspective. By applying the G-mode method, we will search for possible heterogeneities/variegations on the surface characterizing regions with the same spectral behavior. This analysis is therefore fundamental to inferring the formation and evolution of this binary system. Indeed, binary asteroids’ possible compositional differences are

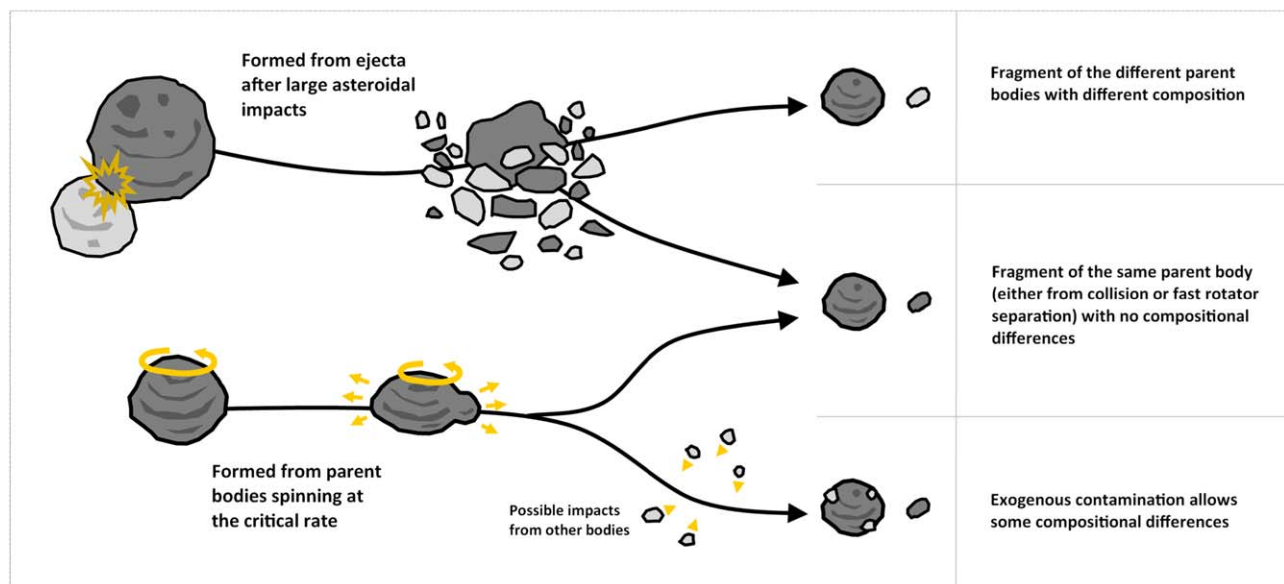


Figure 4. Potential formation scenarios and evolutionary pathways conceivable by LUKE multicolor data. A strong color variation between Didymos and Dimorphos can be associated with formation of the binary system after the catastrophic disruption of parent bodies with compositional differences. The catastrophic scenario can also lead to a binary system with no differences in composition due to formation from fragments of the same parent bodies (or different parent bodies with the same composition). In the case of a binary formation following the disruption of a fast-rotating asteroid, we expect to see no color variation in the LUKE images, although the presence of compositional variation cannot be ruled out due to potential exogenous contamination.

still poorly investigated due to the difficulties of ground-based observation and the absence of dedicated space missions. Nevertheless, the use of general spectrophotometric plots may be adopted to analyze some local regions of interest, as well as the possibility of exploring the spectrophotometric behavior of the data in the RGB colors.

LICIACube, thanks to LUKE observations, will provide the first opportunity to study in detail the possible differences/similarities between the primary asteroid and its moonlet. As summarized in Figure 4, multicolor observations of the two bodies can place strong constraints on the origin of the Didymos–Dimorphos system. In particular, a clear color variation between the two targets can result from a formation scenario followed by a catastrophic disruption of two parent bodies of different compositions. This catastrophic scenario could also lead to a binary system with no differences in composition due to the formation from fragments of the same parent bodies (or different parent bodies with the same composition). In the case of a binary formation following the disruption of a fast-rotating asteroid, we expect to see a smaller color variation in the LUKE images, although the presence of local compositional variation cannot be ruled out due to several conditions, such as a synergic process between topography and space weathering, inhomogeneity inherited from the parent body itself, or potential exogenous contamination from possible asteroids with different composition (DellaGiustina et al. 2021).

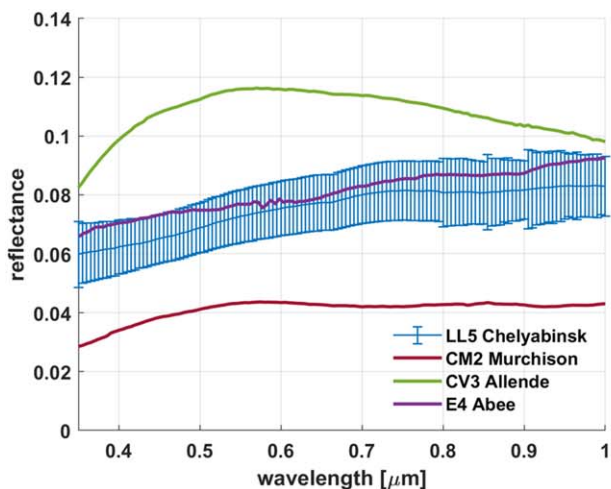
3.2. Laboratory Support of Data Interpretation

Dedicated laboratory analyses will be continuous across all of the LICIACube mission phases to support the interpretation of the data collected by the LICIACube payload. The main activities will concern RGB measurements with LUKE-like RGB cameras and analysis of the LUKE RGB band spectral response with existing and new laboratory spectroscopic measurements in the LUKE wavelength range. In order to

characterize the physical nature of the Didymos system, laboratory studies will provide constraints on albedo, the mineralogical composition for the two asteroids, and the physical properties of the dust plume ejecta compared to what is observed on the surface. Laboratory activities in support of LUKE observations will proceed with two different pathways: (1) the creation of a dedicated database to support the investigation of surface composition and (2) the study of surface processes able to modify the appearance of Didymos’s and Dimorphos’s surfaces.

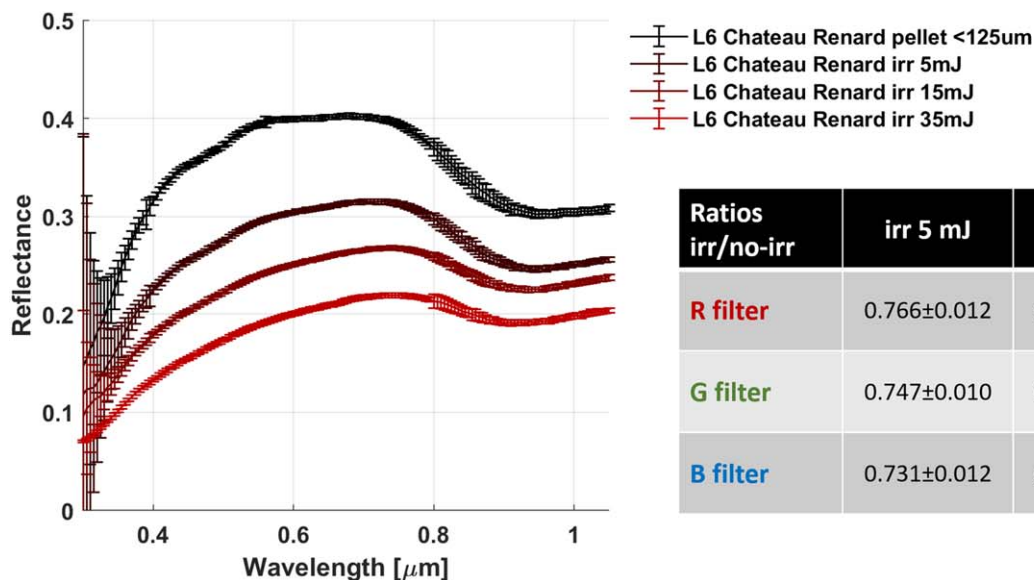
Regarding the database, as shown in Figure 5, different samples will exhibit different values in the RGB band ratios once the VIS spectrum is multiplied to the filters of the LUKE detector and then integrated. Using the band efficiency of the Bayer filter (reported in Figure 2), we are able to extrapolate the possible response of LUKE to several different materials using literature spectra and new measurements. Increasing our knowledge of the response of LUKE to different materials will be achieved by laboratory investigations into the analog conditions of meteorites and natural minerals. Interpreting the possible variation in LUKE data thanks to a broad database including several materials known to be relevant in the main composition of asteroids will help to observe possible differences between the primary and secondary. Acquisition of laboratory spectra and estimation of the instrument throughput of the LUKE filters is ongoing, as is the search in available databases.

A second important activity in the laboratory concerns the study of spectral differences due to physical processes acting on the surface of asteroids. Space weathering is known to be a major source of modification of the visible and infrared appearance of asteroids. Several studies were performed in this field (Lantz et al. 2018; Thompson et al. 2019; Brunetto et al. 2020; just to mention a few of the most recent). Studies of irradiated samples are ongoing to understand how the three bands of the LUKE RGB filters will respond to differences in the surface possibly due to space weathering. As an example,



Meteorite	R/B ratio	R/G ratio
LL5 Chelyabinsk	1.06±0.02	0.92±0.02
CM2 Murchison	1.03	0.89
CV3 Allende	1.01	0.88
E4 Abee	0.96	0.88

Figure 5. Estimation of the instrument throughput of the LUKE filters against relevant samples can help in the interpretation of data collected on the Didymos–Dimorphos system. The left panel shows the VIS–NIR spectra of several meteorites from different classes from the RELAB database (Chelyabinsk C1MT217, Murchison C1MT234A, Allende CAMT230, Abee c1mt40). In the right panel, the ratios of the R band with the other two are reported, and differences in band ratios are linked in differences of composition. The Murchison, Allende, and Abee spectra in RELAB were missing error values, and the Chelyabinsk error is reported for reference as an example of a large laboratory spectrum error. Spectra under acquisition will have lower errors.



Ratios irr/no-irr	irr 5 mJ	irr 15 mJ	irr 35 mJ
R filter	0.766±0.012	0.636±0.009	0.509±0.009
G filter	0.747±0.010	0.609±0.008	0.480±0.008
B filter	0.731±0.012	0.588±0.009	0.453±0.008

Figure 6. Evaluating RGB band ratios among irradiated and pristine surfaces can help in the estimation of the maturity of a surface altered by space weathering. The observation of the DART impact site can unveil the nature of the asteroid composition and surface evolution or even help recognize any other impact crater or feature not previously known or visible with other investigation methods. The spectra used in the example are retrieved from the RELAB database (spectrum code according to the figure legend: C1OC11D, C1OC11D05, C1OC11D15, C1OC11D35).

the band ratios among irradiated and not irradiated surfaces are reported in Figure 6 for an L6 meteorite from the RELAB database. As is visible in the table, irradiation on the surface induces a modification in the spectrum of the sample and therefore a variation in the relative ratios of the LUKE bands before and after the irradiation. Moreover, concerning the modification of the surface due to physical processes, observation of the impact crater generated by DART or other impact craters could generate a difference in the channels of LUKE. This comparison could even help recognize any other impact crater or feature not previously known or visible with other investigation methods.

As shown in Figure 7 for pyroxene and plagioclase samples from RELAB, the spectra of different materials undergo different modifications after an impact, and these differences

can help in discriminating the starting material. As is visible in the band ratios listed in the text boxes inside the plots, differences in the spectroscopic shock response of different materials can be detected by evaluating the RGB band ratios for each filter before and after the impact or other alteration process. In the case study reported, plagioclase variation in the spectra induced by impact, when coupled with LUKE RGB bands, is linear along the channels (i.e., same values for the ratio of each band pre- and postimpact); on the contrary, pyroxene varies differently in each band ratio, as is visible from the text box in the right panel. Evaluating RGB band ratios before and after an alteration process can give useful hints on the surface composition.

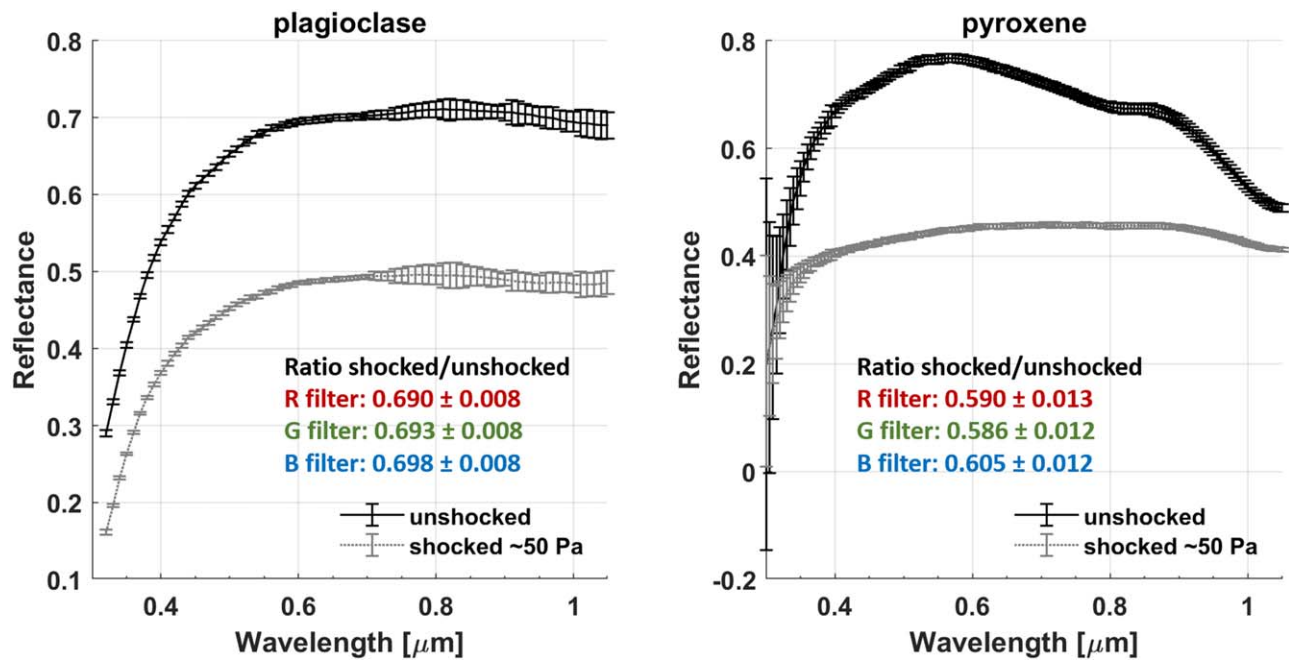


Figure 7. The RGB filter intensity variation can eventually estimate differences in composition due to the impact of the DART spacecraft. In the right and left panels are shown the VIS spectra of two different materials before and after a shock of about 50 GPa (spectra downloaded from RELAB; plagioclase unshocked C1JJ14 and shocked C1JJ26, pyroxene unshocked C1DD74 and shocked C1DD73). As highlighted in the text boxes, differences in the shock response of different materials can be detected by evaluating the RGB band ratios for each filter before and after the impact (or on unaltered/alter surfaces). In this specific case, plagioclase variation in the spectra induced by impact is linear along the three bands (i.e., same values for the ratio of each band pre- and postimpact), while pyroxene varies differently in each band ratio, as is visible from the text box in the right panel.

3.3. Photometric Phase Curve Analysis

During about 10 days in the nominal operation schedule of LICIACube, LUKE is expected to capture images of the Didymos–Dimorphos system ranging from 42° to 120° of phase angle and down to about 51 km (Figure 8). Didymos will become resolved by 4 pixels about 7 minutes before the impact, while Dimorphos will reach the same spatial resolution only 42 s after. The photometric phase curve will reveal some scattering properties of the granular surface medium. With the bidirectional reflectance distribution function (BRDF) reconstructed from these data in combination with ancillary images from SPICE kernel image simulations (Hasselmann et al. 2021; Zinzi et al. 2022), we will be able to undertake disk-resolved photometric modeling (Hapke 2012; Hasselmann et al. 2017, 2021) and apply photometric–topographic corrections (Shkuratov et al. 2011; Li et al. 2015). Within this phase angle coverage, the surface texture, particle irregularities, multiple scattering, and multiscale roughness are the dominant properties (Muinonen et al. 2011; Labarre et al. 2017). In the phase curve, we expect to verify the reflectance increase at larger phase angles; this would indicate the presence or not of the first tail distribution of a forward Henyey–Greenstein lobe (McGuire & Hapke 1995; Munoz et al. 2017). The presence of a forward lobe would help constrain the particle size, as well as understand the limited effect of roughness in the surface. Thus, the photometric modeling is expected to accurately retrieve parameters like average roughness slope and phase function lobe width and ratio (Goguen et al. 2010; Hapke 2012). The photometric phase curve and the BRDF parameters are therefore important physical information for constraining the microphysical properties of simulants and analogs in laboratory experiments (Cord et al. 2003; Jost et al. 2017a, 2017b), aiding the determination of the regolith composition.

3.4. Plume investigations

Images acquired by LICIACube cameras will be pivotal to determine the structure and evolution of the ejecta plume produced by the DART impact. As explained in Dotto et al. (2021), the mission plan was set to allow the spacecraft to achieve the objective of at least three images of the ejecta plume taken over a span of time and phase angle in order to estimate the motion of the slow ($<5 \text{ m s}^{-1}$) ejected particles and study the structure of the plume. In the ejecta observation, LUKE, having a larger FoV with respect to LEIA, will better monitor the evolution of the plume global expansion. Observation of the plume will continue in all subsequent mission phases (Dotto et al. 2021), and the LUKE RGB data, in synergy with the color analysis of the surface, could also be used to investigate the regolith properties and potential heterogeneity (e.g., Perna et al. 2017). Moreover, the LUKE images will allow plume dynamical modeling to predict and constrain the physical and dynamical properties of the expanding ejecta after the impact, as well as provide information on the physical properties on the surface (Ivanovsky et al. 2022, this issue; Rossi et al. 2022).

4. Conclusions

This paper provides an overview of the instrument design, planned operation, and expected performance of LUKE, an RGB camera on board LICIACube, the piggyback cubesat of the NASA DART mission toward the Didymos–Dimorphos binary system. LUKE, along with other cameras in the two spacecraft, will collect several pictures of the asteroids during and after the impact of the DART spacecraft on Dimorphos, performed in order to test the kinetic impactor as a planetary defense technique. Pictures acquired by LUKE will not only

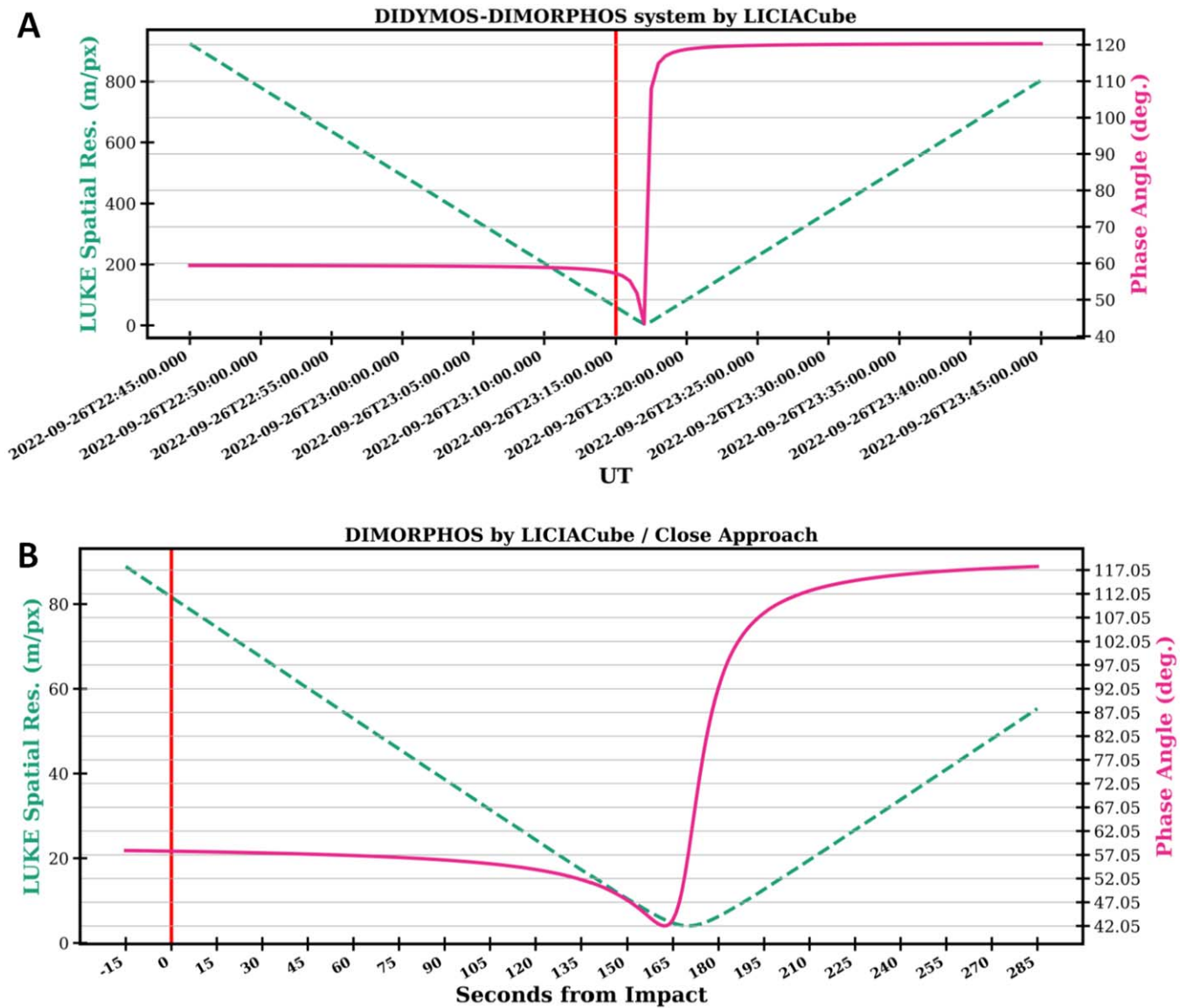


Figure 8. Evolution of the phase angle and spatial resolution of Dimorphos as seen by LUKE/LICIACube. The impact is set at the nominal time of UT 2022 September 26 23:15:45, marked by a red vertical line. (a) Timeline for a window of 30 minutes enclosing the closest approach, from UT 2022 September 26 22:45:00 to UT 2022 September 26 23:45:00. Didymos will become resolved by 4 pixels about 7 minutes before the impact, while Dimorphos will reach the same spatial resolution only 42 s after. (b) LICIACube’s closest approach will be reached 167 s after the impact event. The phase angle will go down to a minimum of $42^{\circ} 10'$ s before LUKE attains the best spatial resolution of 4 m pixel^{-1} for Dimorphos. Didymos’s observational condition will remain favorable until about 240 s after impact (at approximately 40 m pixel^{-1}) but now with a phase angle reaching near 120° .

accomplish the main objective of the mission by possibly observing the plume generated by the DART impact; these data will also allow the science team to infer several physical properties of the asteroid’s surfaces, including information on the composition, morphology, and microphysical properties of the surface. The LUKE data will help improve our knowledge of asteroid binary systems, in particular, their origin and evolution. The expected results promise to significantly advance our understanding of these small rocky bodies in combination with the other data obtained by the mission both from the spacecraft and from ground observations.

The LICIACube team acknowledges financial support from Agenzia Spaziale Italiana (ASI; contract No. 2019-31-HH.0 CUP F84I190012600). This work utilizes spectra downloaded by the NASA RELAB facility at Brown University. All of the

authors have contributed to the present work. The entire LICIACube Team made this paper possible. The authors declare that they have no known competing financial interests or personal relationships that could have appeared to influence the work reported in this paper.

ORCID iDs

Giovanni Poggiali <https://orcid.org/0000-0002-3239-1697>
 John R. Brucato <https://orcid.org/0000-0002-4738-5521>
 Simone Ieva <https://orcid.org/0000-0001-8694-9038>
 Davide Perna <https://orcid.org/0000-0002-4545-3850>
 Maurizio Pajola <https://orcid.org/0000-0002-3144-1277>
 Alessandro Rossi <https://orcid.org/0000-0001-9311-2869>
 Stavro L. Ivanovski <https://orcid.org/0000-0002-8068-7695>
 Angelo Zinzi <https://orcid.org/0000-0001-5263-5348>

Gabriele Cremonese  <https://orcid.org/0000-0001-9021-1140>

Massimo Dall’Ora  <https://orcid.org/0000-0001-8209-0449>

Pasquale Palumbo  <https://orcid.org/0000-0003-2323-9228>

References

- Arakawa, M., Saiki, T., Wada, K., et al. 2020, *Sci*, **368**, 67
- Barucci, M. A., Capria, M. T., Coradini, A., & Fulchignoni, M. 1987, *Icar*, **72**, 304
- Barucci, M. A., Belskaya, I. N., Fulchignoni, M., & Birlan, M. 2005, *AJ*, **130**, 1291
- Barucci, M. A., Hasselmann, P. H., Fulchignoni, M., et al. 2019, *A&A*, **629**, A13
- Barucci, M. A., Hasselmann, P. H., Praet, A., et al. 2020, *A&A*, **637**, L4
- Brunetto, R., Lantz, C., Nakamura, T., et al. 2020, *Icar*, **345**, 113722
- Cheng, A. F., Rivkin, A. S., Michel, P., et al. 2018, *PSS*, **157**, 104
- Cord, A. M., Pinet, P. C., Daydou, Y., & Chevrel, S. D. 2003, *Icar*, **165**, 414
- DellaGiustina, D. N., Burke, K. N., Walsh, K. J., et al. 2020, *Sci*, **370**, eabc3660
- DellaGiustina, D. N., Kaplan, H. H., Simon, A. A., et al. 2021, *NatAs*, **5**, 31
- Deshapriya, J. D. P., Barucci, M. A., Fornasier, S., et al. 2018, *A&A*, **613**, A36
- Deshapriya, J. D. P., Perna, D., Bott, N., et al. 2021, *EPSC*, **2021**, 614
- Dotto, E., Della Corte, V., Amoroso, M., et al. 2021, *PSS*, **199**, 105185
- Fornasier, S., Hasselmann, P. H., Barucci, M. A., et al. 2015, *A&A*, **583**, A30
- Gavrishin, A. I., Coradini, A., & Cerroni, P. 1992, *EM&P*, **59**, 141
- Goguen, Jay D., Stone, Thomas C., Kieffer, Hugh H., & Buratti, Bonnie J. 2010, *Icar*, **208**, 548
- Hapke, B. 2012, *Theory of Reflectance and Emittance Spectroscopy* (2nd ed.; Cambridge: Cambridge Univ. Press),
- Hasselmann, P. H., Barucci, M. A., Fornasier, S., et al. 2017, *MNRAS*, **469**, S550
- Hasselmann, P. H., Fornasier, S., Barucci, M. A., et al. 2021, *Icar*, **357**, 114106
- Honda, R., Arakawa, M., Shimaki, Y., et al. 2021, *Icar*, **366**, 114530
- Ivanovski, S. L., Lucchetti, A., Zanotti, G., et al. 2022, *PSJ*, submitted
- Jost, B., Pommerol, A., Poch, O., et al. 2017a, *PSS*, **145**, 14
- Jost, B., Pommerol, A., Poch, O., et al. 2017b, *PSS*, **148**, 1
- Koga, S. C., Sugita, S., Kamata, S., et al. 2018, *Icar*, **299**, 386
- Labarre, S., Ferrari, C., & Jacquemoud, S. 2017, *Icar*, **290**, 63
- Lantz, C., Binzel, R. P., & DeMeo, F. E. 2018, *Icar*, **302**, 10
- McGuire, A. F., & Hapke, B. W. 1995, *Icar*, **113**, 134
- Michel, P., Kueppers, M., Sierks, H., et al. 2018, *AdSpR*, **62**, 2261
- Muinonen, K., Parviainen, H., Näränen, J., et al. 2011, *A&A*, **531**, A150
- Munoz, O., Moreno, F., Vargas-Martín, F., et al. 2017, *ApJ*, **846**, 85
- Pajola, M., Barnouin, O. S., Lucchetti, A., et al. 2022, *PSJ*, submitted
- Perna, D., Fulchignoni, M., Barucci, M. A., et al. 2017, *A&A*, **600**, A115
- Pravec, P., Scheirich, P., Kušnirák, P., et al. 2006, *Icar*, **181**, 63
- Rivkin, A. S., Chabot, N. L., Stickle, A. M., et al. 2021, *PSJ*, **2**, 173
- Rossi, A., Marzari, F., Brucato, J. R., et al. 2022, *PSJ*, **3**, 228
- Scheirich, P., & Pravec, P. 2009, *Icar*, **200**, 531
- Shkuratov, Y., Kaydash, V., Korokhin, V., et al. 2011, *P&SS*, **59**, 1326
- Sugita, S., Honda, R., Morota, T., et al. 2019, *Sci*, **364**, eaaw0422
- Tatsumi, E., Domingue, D., Hirata, N., et al. 2018, *Icar*, **311**, 175
- Thompson, M.S., Loeffler, M.J., Morris, R.V., et al. 2019, *Icar*, **346**, 113775
- Zinzi, A., Della Corte, V., Ivanovski, S., et al. 2022, *PSJ*, **3**, 126